DOI: http://dx.doi.org/10.32571/ijct.1384351 **E-ISSN: 2602-277X**

International Journal of Chemistry and Technology

http://dergipark.org.tr/ijct

Research Article

Dissolution behavior and kinetic investigation of Mg^{2+}in solution in the reaction of colemanite ore with propionic acid

Mücahit UĞUR[1], Merve DURMAZ[1], M. Muhtar KOCAKERİM[1], Ahmet YARTAŞI[1]*

[1]*Department of Chemical Engineering, Faculty of Engineering, Çankırı Karatekin University, Çankırı 18100, Türkiye*

Received: 1 November 2023; Revised: 17 August 2024; Accepted: 24 August 2024

*****Corresponding author e-mail: m.ugur@karatekin.edu.tr.

Citation: Uğur, M.; Durmaz, M.; Yartaşı, A.; Kocakerim, M.M., *Int. J. Chem. Technol.* **2024**, 8(2), 143-.152.

ABSTRACT

Colemanite ore, which is one of the most significant commercially substantial boron minerals, is used to produce various boron compounds in the industry with its rich B_2O_3 content. Calcium propionate, used in the food industry, is formed as a by-product in its production. In the production of boric acid from colemanite, the use of different solvent reagents is at the forefront to prevent the formation of Mg^{2+}, Ca^{2+} and SO_4^{2-} impurities and borogypsum by-products. For this reason, in our study, the dissolution kinetics of colemanite ore in propionic acid solution in an aqueous medium were carried out in a batch reactor system. As dissolution parameters; reaction temperature, solid/liquid ratio, propionic acid (CH_3CH_2COOH) concentration, stirring speed and particle size were selected. According to the experimental results, the amount of Mg^{2+} passed to the solution; increased; with increase in the reaction temperature, with decrease in solid-liquid ratio, grain size, and acid concentration. In addition, it was determined that the mixing speed was ineffective. Obtained experimental data were analyzed according to homogeneous and heterogeneous reaction models using the Statistica 10.0 package program. It was determined that the dissolution kinetic of Mg^{2+} passing to solution conformed to the "Avrami model" and activation energy (E) was calculated as 8.18 $kJ.mol^{-1}$.

Keywords: Colemanite, propionic acid, dissolution kinetics, heterogeneous reaction.

1. INTRODUCTION

Boron mineral is one of the most significant ores in the world, both strategically and industrially[1]. Boron exists in the form of natural compounds containing different amounts of boroxide (B_2O_3) in their structures[2]. Although there are more than 230 free boron minerals in nature, a few ores such as tincal ($Na_2O.2B_2O_310H_2O$), kernite ($Na_2B_4O_74H_2O$), ulexite ($Na_2O_2CaO_5B_2O_316H_2O$), and colemanite ($Ca_2B_6O_{11}.5H_2O$) which have a monoclinic crystal structure with calcium structure, are top among commercially important ones in the world[3,5]. Since Turkey has about 73% of the worlds' boron deposit, it is important to contribute to make value out it [6,8]. Boron and boron minerals are used in hundreds of different sectors, especially in fiberglass, borosilicate glass [9, 10], high-quality steel, heat-resistant polymers[11], nuclear technology products[1] and rocket engine fuel[12], rubber and paint processing[6], in the field of medicine[13] for the preparation of disinfectants and drugs.

In the production of boron compounds, various studies have been carried out on the dissolution of boron ores in different acidic gas and solution environments. In the literature, the activation energies, leaching solutions and rate control steps of these dissolution processes have been determined [6]. The dissolution of colemanite ore in different reactants occupies a wide area in the literature. SO_2 [14-17], ammonium chloride[18], H_2SO_4 [19-21], methanol [11], potassium dihydrogen phosphate[22], ammonium carbonate [23], ammonium hydrogen sulfate[6], ammonium sulfate [24], perchloric acid [25], citric acid [26], oxalic acid[12], acetic acid [27], chlorine gas [28] were used to dissolve the colemanite ore. In all these studies, we can say that the product film layer on the surface of the ore affects the

DOI: http://dx.doi.org/10.32571/ijct.1384351 **E-ISSN: 2602-277X**

reaction rate and mechanism according to the kind and properties of the reactant used. *Kum et al.* [18] investigated the dissolution kinetics of colemanite ore calcined at 400°C in ammonium chloride solution according to the homogeneous model, and it was determined that the dissolution rate of the process was controlled by the second-order homogeneous reaction model. The activation energy value of the reaction was calculated as $80\ kJ.mol^{-1}$. *Çavuş and Kuşlu*[26] investigated the dissolution kinetic models of colemanite in citric acid solutions with both mechanical shaking and microwave experiment systems. It has been observed that dissolution in the process is controlled by diffusion from the product (ash) film. The activation energy of reactions; was calculated as $28.65\ kJ.mol^{-1}$in mechanical shaking and $21.08\ kJ.mol^{-1}$ in the microwave study. *Gür and Alkan*[25] investigated the solubility of colemanite ore in an aqueous perchloric acid solution in a batch reactor and it was found that the mixing speed was ineffective. It has been determined that the dissolution kinetics is controlled by chemical reactions. *Guliyev et al.*[6] investigated the dissolution kinetics of colemanite in ammonium hydrogen sulfate solutions and determined an alternative reagent to produce boric acid. It was observed that the dissolution rate increased with increasing reaction temperature and decreasing solid/liquid ratio. The activation energy was calculated as $32.66\ kJ.mol^{-1}$. The dissolution rate of the reaction was determined to be controlled by product film diffusion. *Künkül et al.*[23] in this study, the dissolution kinetics of colemanite calcined in ammonium carbonate solutions in a batch reactor was investigated. It was observed that the dissolution rate of the calcined samples was higher than that of the uncalcined sample. It was determined that calcium carbonate did not form on the particle surface. The dissolution kinetics of the process were examined using both heterogeneous and homogeneous reaction models, and it was found that the reaction fit the first-order pseudo-homogeneous reaction model. *Bayca et al.*[29] dissolved colemanite waste in oxalic acid solutions in a batch reactor and it was observed that the process was controlled by a first-order pseudo-homogeneous model. Characterization of colemanite waste was determined by X-Ray diffraction and X-Ray Fluorescence analysis. The activation energy value was obtained as $27.8\ kJ.mol^{-1}$. *Kızılca and Çopur*[11] in the study of, the dissolution of colemanite in methanol investigated in the pressure reactor. Observed that the dissolution rate increased with increase in reaction pressure, temperature, decrease in particle size and solid-liquid ratio. It was observed that the mixing speed had no effect on the dissolution rate, and it was found that the reaction followed the second-order pseudo-homogeneous reaction model. *Karagöz and Kuşlu*[22] investigated the dissolution kinetics of colemanite in potassium dihydrogen phosphate solution and it was determined that the dissolution rate was controlled by a chemical reaction controlled model. It was observed that the dissolution rate of colemanite increased with increasing reaction temperature and KH_2PO_4 concentration, with decreasing solid-liquid ratio and particle size. The activation energy was calculated as $41.88\ kJ.mol^{-1}$.

Industrial boric acid production is achieved according to Equation 1 from the reaction of colemanite with sulfuric acid at approximately 92 °C under atmospheric pressure.

$$Ca_2B_6O_{11}5H_2O + 2H_2SO_4 + 6H_2O \rightarrow 6H_3BO_3 + 2CaSO_4\,2H_2O \quad (1)$$

Various problems occur in the industrial production of boric acid. The main problem in the process is that the by-product borogypsum (gypsum), which can be separated by filtration, is released into the environment and causes soil and environmental pollution[6, 22, 30]. The by-product creates difficult situations in reaction and filtration also causes loss of boron substance in its structure [31]. In addition, it comes from the breakdown of sulfuric acid, which is a strong acid, not only of colemanite ore but also of clay minerals containing some metals such as calcium and magnesium. This situation causes the boric acid produced to be high in terms of calcium, magnesium, and sulfate impurities and reduces the quality of boric acid. Therefore, the use of propionic acid is considered to be applicable since it does not impose an extra economic burden to remove impurities in the product and provides significant advantages in the production of purer boric acid. In addition, the dissolution temperature of colemanite is between 88-92 °C and the vapor pressure of propionic acid is lower than other acids during the reaction, which provides an advantage in terms of acid loss and odor problems[32].

For this reason, the aim of the present research was to examine the kinetics of Mg^{2+}dissolution of colemanite in the presence of propionic acid in the aqueous medium and to determine the reactant that will be an alternative in terms of eliminating the problems encountered in production and product. With the dissolution of colemanite in a propionic acid solution, boric acid and calcium propionate $Ca(CH_3CH_2COO)_2$ as a by-product are formed. Calcium propionate, which has commercial value, is widely used both as a preservative in bakeries and bread and in the food industry to protect bacteria and fungi[33].

The dissolution kinetics of colemanite ore in propionic acid solutions were investigated according to homogeneous and heterogeneous reaction models. In our study; reaction temperature, propionic acid concentration, stirring speed, $solid/liquid$ ratio and grain size of colemanite were chosen as parameters. In the literature, there are no studies on the dissolution behavior and kinetics of Mg^{2+} in solution. There is no literature study on the dissolution behavior and kinetics of Mg^{+2} passing into solution from the clay structures

DOI: http://dx.doi.org/10.32571/ijct.1384351 E-ISSN: 2602-277X

originating from dolomite ($CaCO_3.MgCO_3$) and Mg^{+2}in the structure of colemanite. In addition, there is no study on the ion behavior in the dissolution of colemanite with propionic acid. For this reason, it is thought that examining the parameters' effect in propionic acid solutions will contribute to the literature.

2. EXPERIMENTAL SECTION

2.1. Materials

The colemanite ore used in the study was obtained from the boron deposits of Eti Maden Work in the Emet-Kütahya-Turkey region. After crushing the ore with a crusher, it was ground with a Restch AS200 laboratory grinder and separated into 4 different fractions as 100-150 µm, 150-250 µm, 250-400 µm and 400-600 µm with ASTM sieves. The colemanite used in the experiments was kept in an oven at 105°C for 60 minutes to remove moisture from the ore. The propionic acid, mannitol, NaOH, and HCl used in the study were 99% pure and were obtained from Merck companies. The chemical analysis of the raw ore used in the study was determined by spectrophotometric and gravimetric methods, and the results are recorded in Table 1.

Table 1. The chemical composition of the colemanite ore used in the study.

Comp.	B_2O_3	CaO	H_2O	MgO	Moisture	Others
%	34.2	19.2	14.6	1.72	0.71	29.4

The phase composition of the raw colemanite ore was determined by FEI brand Quanta Feg 250 model X-Ray diffraction (XRD) device and the basic composition of colemanite was determined by Leo 1430 VP scanning electron microscope (SEM) and is given in Figure 1. and Figure 2. respectively.

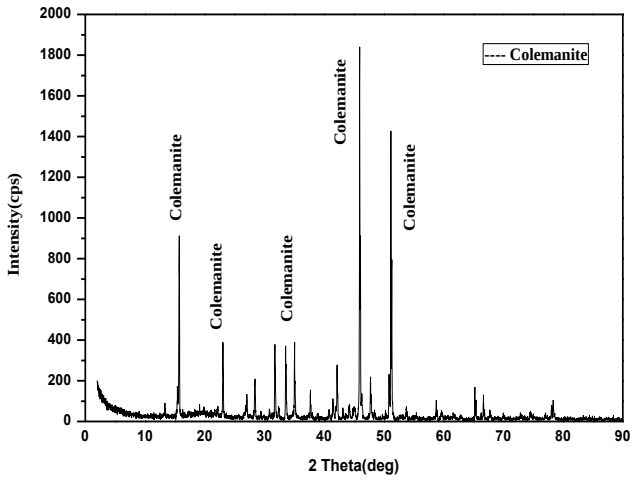

Figure 1. XRD analysis of colemanite ore.

2.2. Methods and experimental procedure

The levels of the parameters used in the kinetic studies were determined as a result of the preliminary trials and literatüre review and are given in Table 1. While examining the effect of a parameter on dissolution kinetics fixed parameters indicated with an asterisk (*) in Table 1 were used to see the effect of the parameters. The grain size is given in Table 2. in the form of two size ranges, and the arithmetic average of these grain sizes is taken in the kinetic calculations. The experimental design plan prepared accordingly is given in Appendix 1.

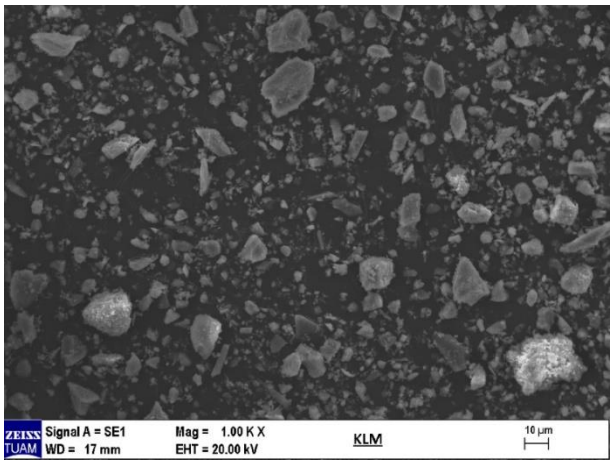

Figure 2. SEM images of colemanite ore.

Table 2. Selected parameters and their levels in the examination of Mg^{2+} kinetics in solution.

	Parameter	Levels
A	Reaction temperature, (°K)	283, 293, **303*,**313, 323
B	Solid/liquid ratio, (g/L)	20, **40***, 60, 80
C	Grain size, (µm)	100-150, 150-250, **250-400***, 400-600
D	Acid Concentration, (M)	4,05-**5,4***-6,75-8,1
E	Stirring speed, (rpm)	300, **400***, 500

*Parameter that remains constant while examining the effect of another parameter

In this study, the dissolution process was carried out under atmospheric pressure and the experimental setup used in the dissolution process is shown in Figure 3. A constant temperature circulator of the brand Polyscience SD20R-30-12EA was used to keep the internal temperature of the reactor at a constant value. In addition, to ensure the homogeneity of the solution in the reactor, a Scilogex OS20-Pro brand mechanical mixer with a tachometer was used.

For kinetic studies, a propionic acid-water solution with a certain solid/liquid ratio was taken into the 500 mL double-walled glass reactor. After the propionic acid suspension reached the desired temperature for the

DOI: http://dx.doi.org/10.32571/ijct.1384351 E-ISSN: 2602-277X

reaction using a temperature circulator, colemanite ore was added and the reaction started. During the 60-minute experiment, samples were taken from 11 reaction solutions at certain intervals

2.3. Analysis and modeling

The amount of Mg^{2+} transferred to the aqueous solution in the samples taken at regular intervals throughout the experiment was determined with the help of an AAS (Atomic Absorption Spectrophotometer) and expressed as a percentage. Dissolution percentage values were used in kinetic modeling using the Statistica 10 package program. The exponential constants (a, b, c, m) and the regression coefficient (r^2) in the kinetic model were calculated statistically with the Statistica 10 package program, and the Arrhenius constant (A) and the activation energy (E) were calculated from the Arrhenius plot.

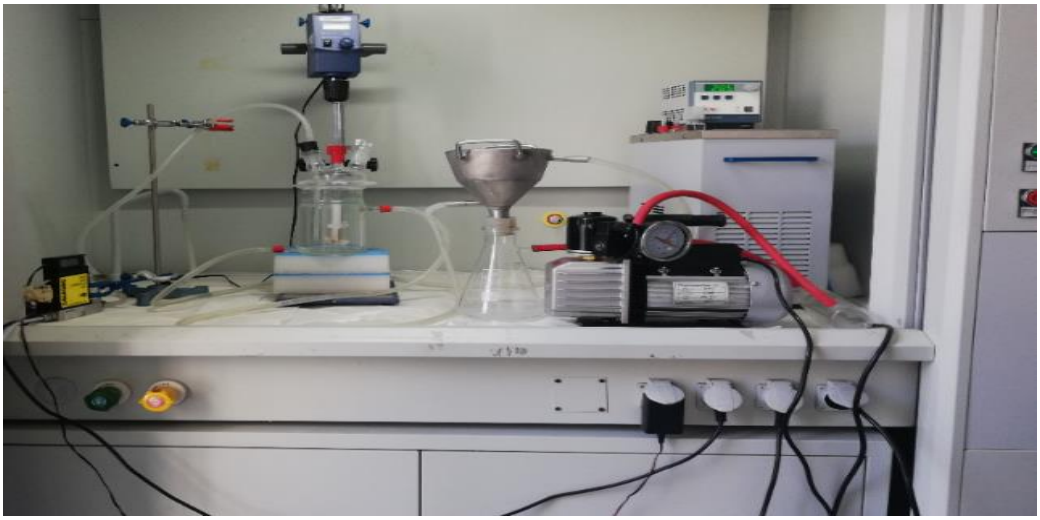

Figure 3. The experimental setup used in our experimental studies.

3. RESULTS AND DISCUSSION

3.1. Reactions for kinetic solutions

The ionization reaction of propionic acid in an aqueous solution can be written as:

$$4CH_3CH_2COOH_{(aq)} + 4H_2O_l \rightarrow 4CH_3CH_2COO^-_{(aq)} + 4H_3O^+_{(aq)} \quad (1)$$

When colemanite is added to the propionic acid solution, the reactions occurring in the medium is as follows;

$$2CaO.3B_2O_3.5H_2O_{(s)} + 2H_3O^+_{(aq)} \rightarrow Ca^{2+}_{(aq)} + 2H_3BO_{3(aq)} + CaO.2B_2O_{3\,(k,aq)} + 4H_2O_{(l)} \quad (2)$$

$$CaO.2B_2O_{3\,(k,aq)} + 2H_3O^+_{(aq)} \rightarrow Ca^{2+}_{(aq)} + 2H_3BO_{3(aq)} \quad (3)$$

$$Ca^{2+}_{(aq)} + CH_3CH_2COO^-_{(aq)} \rightarrow Ca(CH_3CH_2COO) \quad (4)$$

The overall reaction is as follows;

$$2CaO.3B_2O_35H_2O_{(s)} + 4CH_3CH_2COOH_{(aq)} + 2H_2O \rightarrow 2Ca^{2+}_{(aq)} + 6H_3BO_{3\,(aq)} + 4CH_3CH_2COO^-_{(aq)} \quad (5)$$

3.2. Effect of parameters

During the dissolution of colemanite ore in propionic acid solutions under atmospheric pressure; the effects of reaction temperature, solid-liquid ratio, particle size, propionic acid concentration, and stirring speed parameters on the dissolution of Mg^{2+}were investigated. The experimental results obtained using the parameters and levels given in Table 2. are plotted as the percent dissolution of Mg^{2+} versus time.

3.2.1.Effect of reaction temperature

Temperature is one of the most important factors for dissolution kinetics. The effect of reaction temperature on the rate of dissolution of Mg^{2+}in solution was investigated at 283, 293, 303, 313 and 333°K. The graph of the obtained dissolution percentages versus time is given in Figure 4. Since the kinetic energy increases exponentially with the increase of the reaction temperature, the number of collisions of the molecules per unit of time also increases[8, 29]. For this reason, it is seen that the reaction rate increases with the increase in temperature, and therefore the amount of Mg^{2+} that passes into the solution in the aqueous medium increases.

DOI: http://dx.doi.org/10.32571/ijct.1384351 E-ISSN: 2602-277X

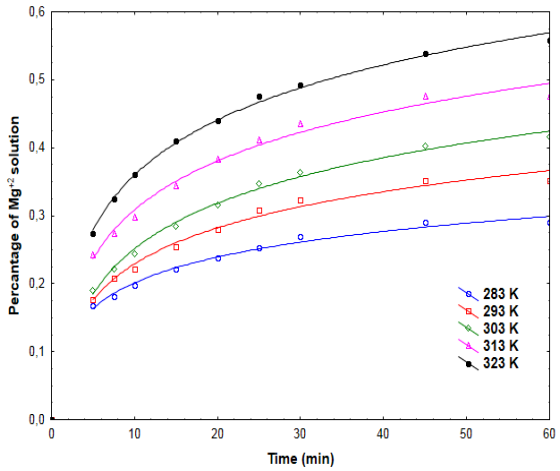

Figure 4. The effect of reaction temperature on the passing of Mg^{2+}into the solution.

3.2.2.Effect of particle size

The effect of particle size on the dissolution rate of $Mg^{2+}$was investigated in the size ranges of 100-150, 150-250, 250-400, and 400-600 µm. The percentage of dissolution graphs obtained against time is given in Figure 5. Reducing the particle size increases the total surface area in the solution. As the surface area increases, naturally, the dissolution surface per unit amount of solvent also increases. Therefore, it is an expected result that the dissolution rate of Mg^{2+}increases as the particle size decreases.

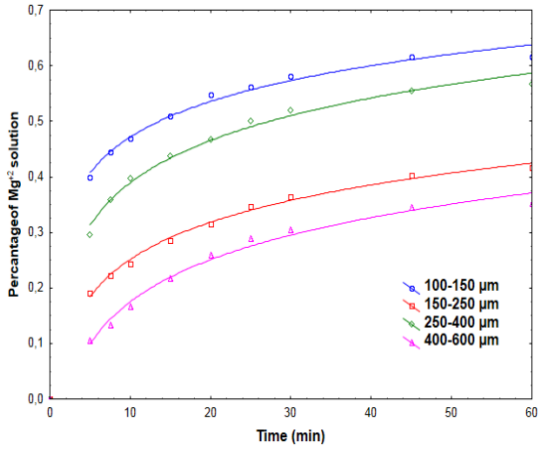

Figure 5. The effect of grain size on the passing of $Mg^{2+}$the into the solution.

3.2.3.Effect of solid-liquid ratio

The effect of solid/liquid ratio on the rate of Mg^{2+}passing into solution; was examined using values of 20, 40, 60 and 80 $g.L^{-1}$. The percentage of dissolution graphs obtained against time is given in Figure 6. As seen in Figure 6., it is seen that the dissolution rate of Mg^{2+}decreases with the increase in the solid/liquid ratio. The increase in the solid/liquid ratio causes a decrease in the dissolution rate of Mg^{2+}, an increase in the amount of solid per unit solvent, and a decrease in the rate and amount of Mg^{2+}. Similar results were observed in the dissolution of colemanite ore in methanol and ammonium hydrogen sulfate solutions [6, 11].

3.2.4.Effect of acid concentration

The effect of propionic acid concentration on the rate of Mg^{2+} in solution was examined as 4.05, 5.4, 6.75 and 8.1 M. Time versus dissolution percentage values are given graphically in Figure 7. As can be seen in Figure 7, the rate of Mg^{2+} in solution decreases as the acid concentration increases. As the acid concentration increases, the reactants collide more per unit time, so the reaction takes place more quickly and less dissolution of the colemanite particles is ensured.

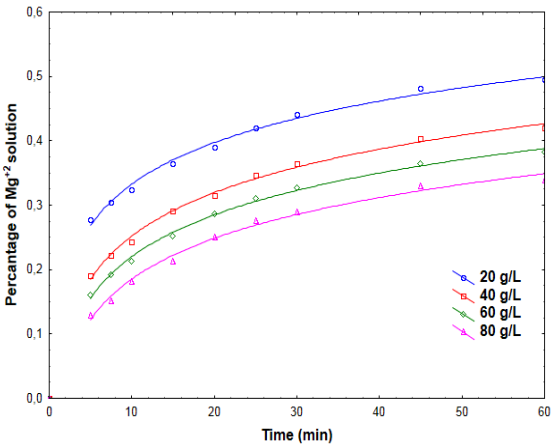

Figure 6. The effect of solid/liquid ratio on the passing of Mg^{2+}into the solution.

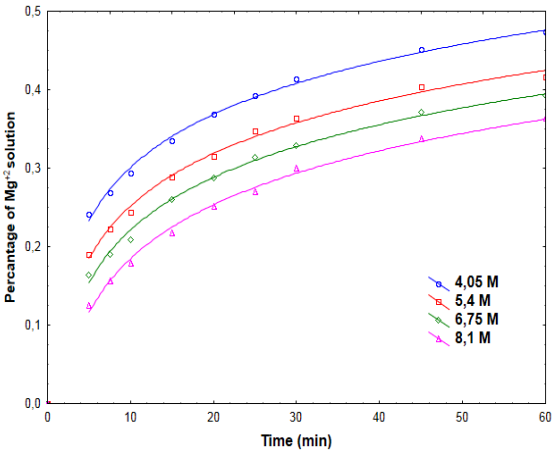

Figure 7. Effect of propionic acid concentration on Mg^{2+}passing into the solution.

3.2.5.Effect of mixing rate

The effect of the mixing speed on the dissolution rate of Mg^{2+} was investigated at mixing speeds of 300, 400 and 500 rpm. The effect of propionic acid concentration on the rate of dissolution Mg^{2+}in solution versus

DOI: http://dx.doi.org/10.32571/ijct.1384351 E-ISSN: 2602-277X

dissolution percentage values is given graphically in Figure 8. As shown in Figure 8., the mixing speed does not significantly contribute to the dissolution percentage of Mg^{2+}. Since the mixing speed was not effective, the mixing speed data were not used in the calculation of the kinetic model equation.

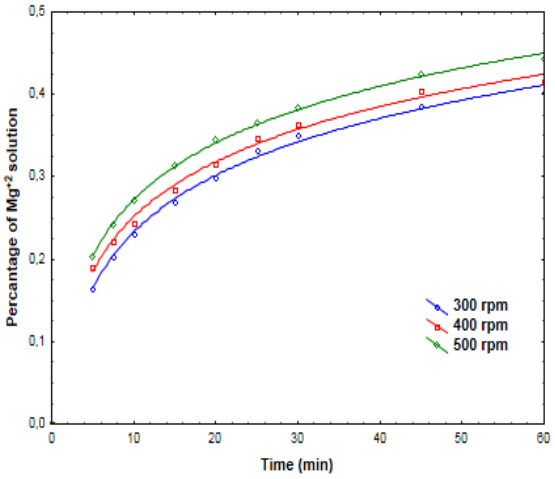

Figure 8. The effect of mixing speed on Mg^{2+} passing into the solution.

3.3. Kinetic analysis

Solid-liquid reaction rates can be explained according to heterogeneous and homogeneous reaction models [34]. In the homogeneous reaction model, a reactant liquid is assumed to enter the particle and form a reaction throughout the particle. In the heterogeneous model, the reaction is considered to take place on the outer surface of the unreacted particle.

3.3.1.Determination of the kinetic model

The solution kinetics of Mg^{2+} during the dissolution of colemanite ore in aqueous propionic acid solutions has been tried to be explained using homogeneous and heterogeneous reaction models. Experimental results were evaluated graphically and statistically. To determine with which rate equation this process is controlled, the reaction rate equations were tried one by one according to the control mechanisms by using the solubility percentage values of all factors for Mg^{2+} and the r^2 (regression) values are given in Table 3.

Considering that the steps controlling the rate are the ones controlling the reaction rate with the highest resistance, the Avrami model was determined to be the most appropriate model and a kinetic model representing the process was derived by considering the effects of the parameters. The reaction rate expression according to the Avrami model is given in Equation 6:

$$kt^m = -\ln(1 - X) \quad (6)$$

If the logarithm of Equation 6 is taken;

$$\ln k + m \ln t = \ln[-\ln(1-x)] \quad (7)$$

obtained

Table 3. Velocity equations were tried in modeling and r^2 values found.

Hız Denklemleri	Hız Kontrol Modelleri	r^2
$kt^m = \ln(1-X)$	**Avrami**	**0,983**
$kt = 1-3(1-X)^{2/3} + 2(1-X)$	Ash film diffusion controlled for spherical fixed size grains	0,914
$kt = 1-(1-X)^{1/3}$	Chemical reaction controlled	0,228
$kt = 1 - (1-X)^{1/2}$	Fluid film diffusion-controlled for shrinking sphere, large grains	0,612
$kt = 1 - (1-X)^{2/3}$	Fluid film for shrinking sphere with diffusion control, small grains	0,37
$kt = -\ln(1-X)$	First-order pseudo homogenous reaction model	0,485
$kt = X/(1-X)$	Second-order pseudo homogeneous reaction model	0,787
$kt = X^2$	Ash film diffusion control for fixed-size flat plate	0,875
$kt = X + (1-X)\ln(1-X)$	Ash film diffusion control for fixed size cylinder	0,904

The graphs of lnt versus ln[-ln(1-x)] for different temperatures are shown in Figure 9. The lnk values were determined from the intersection values of the lines with the ordinates. It is seen in the graph that each temperature curve forms a line (r^2 values are very close to 1).

DOI: http://dx.doi.org/10.32571/ijct.1384351 **E-ISSN: 2602-277X**

3.3.2.Determination of activation energy and arrhenius constant

The reaction rate constant, k, is determined from the slope of each temperature line in Figure 9. The reaction rate constant is temperature-dependent and is used to determine the relationship between k and T in the Arrhenius equation [35, 36].

$$K = Ae^{-E/RT} \quad (8)$$

Equation 9 is obtained by taking the natural logarithm of both sides of Equation 8.

$$lnk = lnA - E/RT \quad (9)$$

The Arrhenius graph in Figure 10 is obtained by applying the lnk versus $1/T(K)$ graphs for each temperature value.

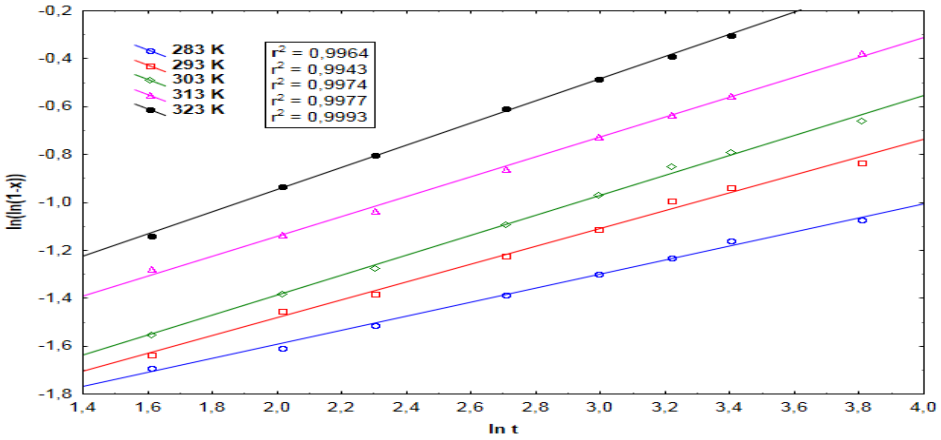

Figure 9. lnt counter-exchange with ln[-ln(1-X)] of different reaction temperatures.

.

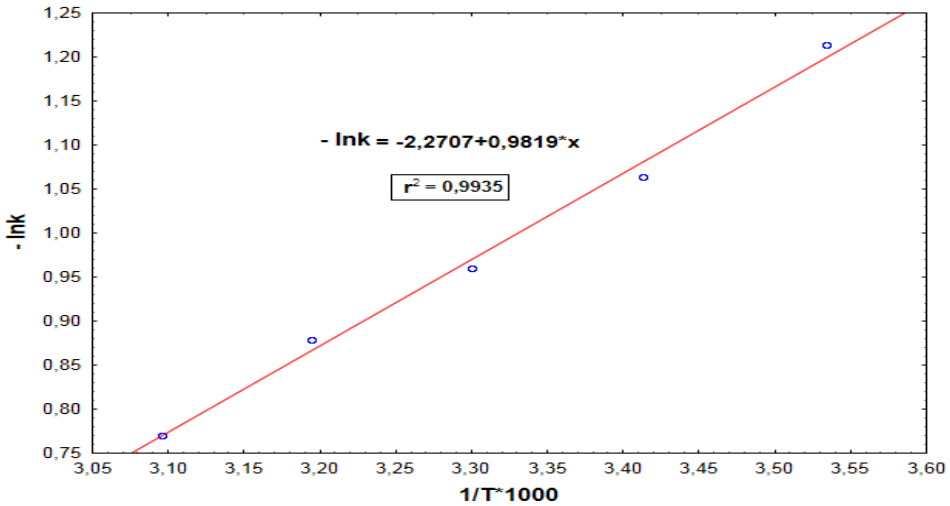

Figure 10. 1/T(K)*1000 versus lnk plot (Arrhenius graph.

From the slope and shear point of the Arrhenius plot, the activation energy (E) was determined as 8.18 kJ/mol and the Arrhenius constant (A) as 9.79. The rate constant (k) in the Avrami model in Equation 6; solid-liquid ratio, particle size and propionic acid concentration dependence are given in Equation 10.

$$k = A(S/L)^a(C)^b(D)^c(W)^d e^{\frac{-E}{RT}} \quad (10)$$

If the rate constant k in Equation 10 is substituted in the Avrami model, Equation 11 is obtained.

$$-ln(1 - X_{Mg^{2+}}) = A(S/L)^a(C)^b(D)^c . e^{\frac{-E}{RT}} t^m \quad (11)$$

DOI: http://dx.doi.org/10.32571/ijct.1384351 E-ISSN: 2602-277X

Here, the exponential constants a, b, c, m were determined using the Statistica 10 package program, statistical calculations with multiple simultaneous regressions, and the activation energy (E) and Arrhenius

constant (A) were determined using the Arrhenius graph. The constants were determined as -0.228, -0.369, -0.49, 0.221 respectively. These results are substituted in Equation 11 and the following "Avrami model equation" is obtained.

$$-\ln\left(1-X_{Mg^{2+}}\right) = 9{,}79.(S/L)^{-0{,}228}(C)^{-0.369}(D)^{-0.49}e^{\frac{-8.18}{R*T}}t^{0.221} \quad (12)$$

According to both statistical and graphical results, it is seen that the rate mechanism controlling the dissolution percentage fits the Avrami model.

3.3.3.Validation of the kinetic model

The theoretical dissolution percentage values of $Mg^{2+}$are in Figure 11. were calculated with the help of Equation 10 in the Statistica 10 package program, and the experimental dissolution percentage values were calculated using the Avrami model equation. Sorting the theoretical percent dissolution and experimental dissolution percentage values on the same diagonal in the graph shows that the experimental and theoretical transformation results of the model chosen for this process are in harmony with each other.

4. CONCLUSIONS

In this study, the solution kinetics of Mg^{2+} in the dissolution of colemanite in propionic acid solution in an atmospheric pressure environment is examined and an alternative reactant for boric acid production is proposed. Parameters and levels were determined in the light of preliminary trials and literature information. Obtained results,

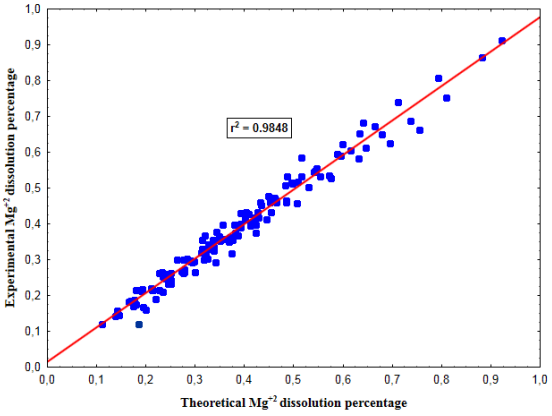

Figure 11. Compatibility of experimental transformation values with theoretical transformation values.

- ✓ The rate of Mg^{2+} passing into the solution increases with the increase in reaction temperature, which increases in parallel with the reaction rate.
- ✓ As the solid-liquid ratio increases, the rate of Mg^{2+} passing into the solution decreases as the amount of solid per unit solvent increases. As the propionic acid concentration increases, the reaction occurs faster as it comes into contact with colemanite more in unit time, and the rate of Mg^{2+}passing into the solution decreases. Due to the increased surface area with the decrease in particle size, the rate of Mg^{2+}passing into the solution increases. It shows that the mixing speed has no significant effect on dissolution.
- ✓ It was determined that propionic acid, which has weak acidic properties compared to H_2SO_4, can dissolve colemanite ore in boric acid production and is an alternative reactant for boric acid production. The by-product (calcium propionate), which is environmentally friendly, soluble in water, has commercial value and is used especially in the food sector, was obtained.
- ✓ Experimental results obtained for the kinetic model of the dissolution rate of Mg^{2+}, which goes into solution in an aqueous medium, were applied to homogeneous and heterogeneous models. It has been found that the Avrami model fits [$-\ln(1-X) = kt^m$]. The activation energy of the process was calculated as 8.18 $kJ.mol^{-1}$ and the Arrhenius constant (A) as 9.79.
- ✓ A mathematical model based on the specified parameters was derived;

$$-\ln\left(1-X_{Mg^{2+}}\right) = 9{,}79.(S/L)^{-0{,}228}(C)^{-0.369}(D)^{-0.49}e^{\frac{-8.18}{R*T}}t^{0.221}$$

ACKNOWLEDGMENTS

This research was carried out with the support of the Scientific Research Project (MF210621D06) funded by Çankırı Karatekin University. Authors are thankful to Çankırı Karatekin University, Scientific Research Project Management Unit (ÇAKÜ-BAP). Determination of the concentration of the elements was achieved made using the Shimadzu AA-7000 Atomic Absorption Spectrophotometer (AAS) device at Çankırı Karatekin University.

Conflict of interest

I declare that there is no a conflict of interest with any person, institute, company, etc.

Nomenclatures

a, b, c, d, m	Model constants
A	Frequency factor
C	Propionic acid concentration (M)
D	Average particle size (µm)
W	Mixing speed (rpm)
E	Activation energy
k	Reaction rate constant

DOI: http://dx.doi.org/10.32571/ijct.1384351 E-ISSN: 2602-277X

L	Liquid amount (mL)
r^2	Regression coefficient
R	Ideal gas constant (8.314 $kJ/kmol.K$)
s	Solid amount (g)
t	Time (min)
T	Temperature (°K)
X	Conversion fraction

Indeces

s	Solid
aq	Aqueous solution
l	Liquid

Table 1. Kinetic study experiment plan.

Experiment No.	Reaction temperature (K)	Particle size (µm)	Solid/fluid ratio (g/L)	Acid concentration (M)	Mixing rate (rpm)
1	**283**	250-400	40	5.4	400
2	**293**	250-400	40	5.4	400
3	**303**	250-400	40	5.4	400
4	**313**	250-400	40	5.4	400
5	**323**	250-400	40	5.4	400
6	303	**100-150**	40	5.4	400
7	303	**150-250**	40	5.4	400
8	303	**400-600**	40	5.4	400
9	303	250-400	**20**	5.4	400
10	303	250-400	**60**	5.4	400
11	303	250-400	**80**	5.4	400
12	303	250-400	40	**4.05**	400
13	303	250-400	40	**6.75**	400
14	303	250-400	40	**8.1**	400
15	303	250-400	40	5.4	**300**
16	303	250-400	40	5.4	**500**

REFERENCES

1. Doğan , H. T.; Yartaşı, A. Hydrometallurgy **2009**, 96 (4), 294-299.
2. Kopac, T.; Kırca,Y.; Toprak, A. Int j hydrogen energy **2017,** 42 (37), 23606-23616.
3. Kucuk, V.; Kocakerim, M. M. Iran j Chem chem eng **2019**, 38 (3), 245-255.
4. Küçük, Ö.; Korucu, H. J chemical Soc pakistan **2018,** 40 (3).
5. Sert, H.; Yıldıran, H.; Toscalı, D. Int j hydrogen energy **2012,** 37 (7), 5833-5839.
6. Guliyev, R.; Kuşlu, S.; Çalban, T.; Çolak, S. J ind eng chem **2012,** 18 (4), 1202-1207.
7. Elçiçek, H.; Kocakerim, M. M. Braz j chem eng **2018**, 35, 111-122.
8. Şimşek, H. M.; Guliyev, R.; Beşe, A. V. Int j hydrogen energy **2018**, 43 (44), 20262-20270.
9. Arasu, A. V.; Sornakumar, T. Sol energy **2007**, 81 (10), 1273-1279.
10. Uğur, M. Rev Mineral **2024,** 9 (1), 9-18 (2024).
11. Kizilca, M.; Copur, M. Chem eng commun **2015**, 202 (11), 1528-1534.
12. Alkan, M.; Doğan, M. Chem eng process **2004** 43 (7), 867-872.
13. Tunc, M. Asian j chem **2008** 20(4):3161-3170.
14. Alkan, M.; Kocakerim, M. M.; Çolak, S. J chem technol biot **1985**, 35 (7), 382-386.
15. Kocakerim, M. M.; Alkan, M. *Hydrometallurgy* **1988,** 19 (3), 385-392.
16. Küçük, Ö.; Kocakerim, M. M.; Yartaşı, A.; Çopur, M. Ind eng chem **2002**, 41 (12), 2853-2857.
17. Kurtbaş, A.; Kocakerim,M. M.; Küçük, Ö.; Yartaşı, A. Ind eng chem **2006,** 45 (6), 1857-1862.
18. Kum, C.; Alkan, M.; Kocakerim, M. M. *Hydrometallurgy* **1994,** 36 (2), 259-268.
19. Temur, H.; Yartaşı, A.; Copur, M., Kocakerim, M. M. Ind eng chem **2000**, 39 (11), 4114-4119.
20. Okur, H.; Tekin, T.; Ozer, A. K.; Bayramoglu, M. *Hydrometallurgy* **2002,** 67 (1-3), 79-86.
21. Gür, A. Korean j chemical eng **2007**, 24 (4), 588-591.
22. Karagöz, Ö.; Kuşlu, S. Int j hydrogen energy **2017**, 42 (36), 23250-23259.

DOI: http://dx.doi.org/10.32571/ijct.1384351 **E-ISSN: 2602-277X**

23. Künkül, A.; Aslan, N. E.; Ekmekyapar, A.; Demirkıran, N. Ind eng chem **2012**, 51 (9), 3612-3618.

24. Tunç, M.; Kocakerim, M. M.; Küçük, Ö.; Aluz, M. Korean j chem eng **2007**, 24 (1), 55-59.

25. Gür, A.; Alkan, M. E. J chem eng jpn **2008**, **41** (5), 354-360.

26. Çavuş, F.; Kuşlu, S. Ind eng chem **2005,** 44 (22), 8164-8170.

27. Özmetin, C.; Kocakerim, M. M.; Yapıcı, S.; Yartaşı, A. Ind eng chem **1996**, 35 (7), 2355-2359.

28. Ceyhun, I.; Kocakerim, M.; Saraç, H.; Çolak, S. Theor found chem eng **1999**, 33 (3).

29. Bayca, S. U.; Kocan, F.; Abali,Y. Environ prog sustain **2014**, 33 (4), 1111-1116.

30. Budak, A.; Gönen, M. J supercrit fluids **2014**, 92, 183-189.

31. Tunc, M.; Irem, H.; Kocakerim, M. M.; Copur, M.; Küçük, Ö. Iran j chem chem eng **2020**, 39 (2), 83-90.

32. Uğur, M. Iran j chemi chem eng **2024**.

33. Phechkrajang, C. M.; Yooyong, S. J food drug anal **2017**, 25 (2), 254-259.

34. O, L.; *Chemical Reaction Engineering*. **1999**; P 566-586.

35. Abanades, S.; Kimura , H.; Otsuka, H. Int j hydrogen energy **2015**, 40 (34), 10744-10755.

36. Naktiyok, J.; Bayrakçeken, H.; Özer, A, K.; Gülaboğlu, M. Ş. Fuel process technol **2013,** 116, 158-164.